

Disentangling the response of forest and grassland energy exchange to heatwaves under idealized land-atmosphere coupling

Chiel C. van Heerwaarden¹ and Adriaan J. Teuling²

¹Max Planck Institute for Meteorology, Hamburg, Germany

²Hydrology and Quantitative Water Management Group, Wageningen University, Wageningen, The Netherlands

Correspondence to: Chiel van Heerwaarden
(chiel.vanheerwaarden@mpimet.mpg.de)

Abstract. This study investigates the difference in land-atmosphere interactions between grassland and forest during typical heat wave conditions in order to understand the controversial results of Teuling et al. (2010) (T10, hereafter), who have found the systematic occurrence of higher sensible heat fluxes over forest than over grassland during heat waves. With a simple, but accurate coupled land-atmosphere model, we are able to reproduce the findings of T10 for normal summer and heat wave conditions, and to demonstrate the sensitivity of the coupled system to changes in incoming radiation and early-morning temperature typical for European heatwaves. Our results emphasize the importance of fast interactions (time scales up to minutes) between vegetation and the atmosphere in creating the differences between grassland and forest. As our parametrization for stomatal resistance is empirical rather than mechanical, our study stresses the demand for a better mechanistic understanding of physiological processes in plants.

In order to disentangle the contributions of differences in several static and dynamic properties between forest and grassland, we have performed a virtual experiment in which new land use types are created that are equal to grassland, but with one of its properties replaced by that of forest. From these, we confirm the important role of the fast physiological processes that lead to the closure of stomata. Nonetheless, for a full explanation of T10's results the other properties (albedo, roughness and the ratio of minimum stomatal resistance to leaf-area index) play an important, but indirect role; their influences mainly consist of strengthening the feedback that leads to the closure of the stomata by providing more energy that can be converted into sensible heat. The model experiment also confirms that, in line with the larger sensible heat flux, higher atmospheric temperatures occur over forest.

1 Introduction

There are strong indications that the intensity and frequency of mid-latitude heat waves has increased over the last decades, but the degree to which this can be attributed to human influence on the climate is uncertain (IPCC, 2013). Since local land surface conditions can strongly impact temperatures during heatwaves (Fischer et al., 2007; Miralles et al., 2012), any changes in land surface conditions, for instance through land use change, have the potential to impact temperature extremes. Probably the most striking example of land-use change in the world is deforestation; in many parts of the world forests have been converted into grassland over the last centuries (e.g., Christidis et al., 2013). Despite the fact that deforestation has been recognized as an important driver of local climate change (Davin and de Noblet-Ducoudré, 2010; Bonan, 2008), its effect on heat waves is still poorly understood. Until now it is unclear whether forests reach higher or lower temperatures than grassland during warm summer conditions or heat waves (Zaitchik et al., 2006; Teuling et al., 2010; Anderson et al., 2010). One of the major open questions is how and to which extent land-use affects temperature extremes during heat waves. This is shown to depend strongly on feedbacks between the land surface and the atmospheric boundary layer (Stap et al., 2014).

The recent study of Teuling et al. (2010) (hereafter T10) showed that during the early stages of a heat wave the sensible heat fluxes above forests can far exceed those over grassland, despite the common belief that forests with their deeper root systems would maintain higher evapotranspiration rates and thus dampen the strength of heat waves (Bonan, 2008). To illustrate this, Figure 1 shows the composite relationship between midday temperature and incoming short wave radiation and the preceding midday (9-12 h UTC)

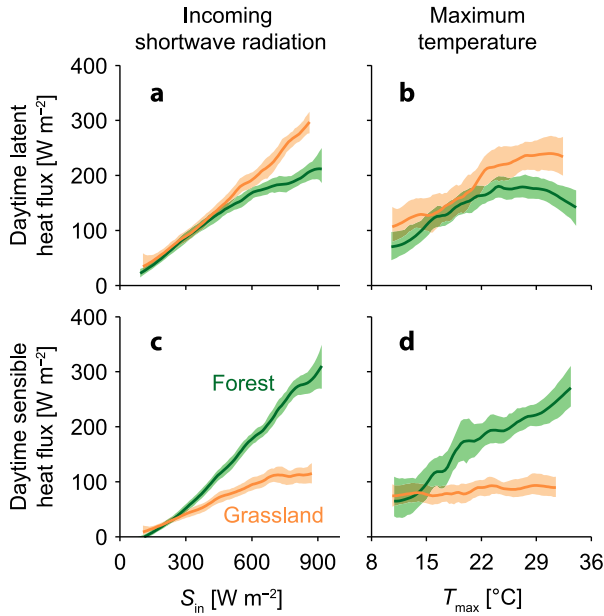


Fig. 1. Observed midday sensible heat fluxes H (a) and latent heat fluxes LE (b) over forest and grassland sites as a function of daily maximum air temperature and averaged incoming shortwave radiation. Curves have been derived using locally weighted polynomial regression (LOESS) on all midday data (9:00–13:00 UTC), heat wave days included, in the months June–August for all European FLUXNET sites analysed in T10. Uncertainty bounds reflect 5% and 95% percentiles of the LOESS regression as determined by bootstrapping. See Supplementary Information in T10 for more information.

sensible and latent heat fluxes over all European forest and grassland FLUXNET sites with long-term observations taken from T10. We can induce from this figure that forest amplifies its near-surface temperature by increasing its sensible heat flux under high temperatures and high incoming shortwave radiation, whereas grassland maintains a more constant flux. This, however does not immediately imply that the highest temperatures occur over forest, as the temperature increase due to the extra sensible heat flux is (partly) offset by increased mixing above the canopy due to the higher roughness of forest. Furthermore, we find that forest has an optimum in the evaporation rate for maximum temperatures between 294 and 300 K, whereas grassland still increases with maximum temperature within this range.

In this paper, we aim at improving our understanding of the mechanisms that drive the behavior reported by T10 and Figure 1 by means of a modeling experiment of the coupled land surface-atmospheric boundary layer system. In order to provide a theoretical framework for our analysis, we start this study by explaining the differences in feedback loops that regulate the atmospheric control on evapotranspiration between forest and grassland (Section 2).

For our modeling experiment we use a coupled model that consists of a bulk schematization for the atmospheric boundary layer, a force-restore land surface scheme, and a basic radiation scheme (van Heerwaarden et al., 2010a,b; Vilà-Guerau de Arellano et al., 2012). The essence of our experiment is that we model a typical day in order to show that the modeling of fast processes is sufficient to explain the first order response of the coupled land-atmosphere system to heat wave conditions. Our focus is thus on short heatwaves, because in longer heat waves the depletion of soil moisture plays an important role (Fischer et al., 2007; Miralles et al., 2014). The relevant fast processes in this study are the atmospheric turbulence, the opening and closure of the stomata of the vegetation, and the response time of the surface temperature, which all have time scales less than tens of minutes. The model and the experiments are described in Section 3. Our modeling experiment consists of three phases.

First, we evaluate our model against observations reported in T10 for normal summer and heat wave conditions (Section 4.1). Then, we perform a sensitivity study on the external forcings and show how the surface energy balance, atmospheric temperature and humidity and the boundary layer height respond to changes in the incoming radiation and the large scale temperature forcing (Section 4.2). To conclude, we analyze the differences between forest and grassland in detail, by comparing the relative importance of properties of the land surface that are different between forest and grass: the albedo, the physiological response of the vegetation, the ratio of the leaf-area-index to the minimum resistance and the roughness (Section 4.3).

In our model, we represent the response of the vegetation to the atmosphere in an empirical way (Jarvis, 1976), similar as the implementation in the majority of the numerical weather prediction models (e.g. Noilhan and Mahfouf, 1996; Ek et al., 2003). Although these models have been tuned to give a good performance over Europe, the parametrization is not mechanical. The mechanisms within the plant that drive the response to the air temperature and vapor pressure deficit are still poorly understood (Monteith, 1995) and contradicting descriptions can be found in the literature (Streck, 2012). Although Oren et al. (1999) shows that many leaf stomata reduce their aperture under the presence of dry air, studies at the landscape scale show for instance maintained evapotranspiration during dry spells in mountainous grasslands (Brilli et al., 2011). In addition, detailed measurements among different crops show very species specific behaviour (van de Boer et al., 2014). Our study will therefore focus on the relative importance of the combined physiological response of the vegetation to temperature and humidity in comparison to the other more static vegetation properties.

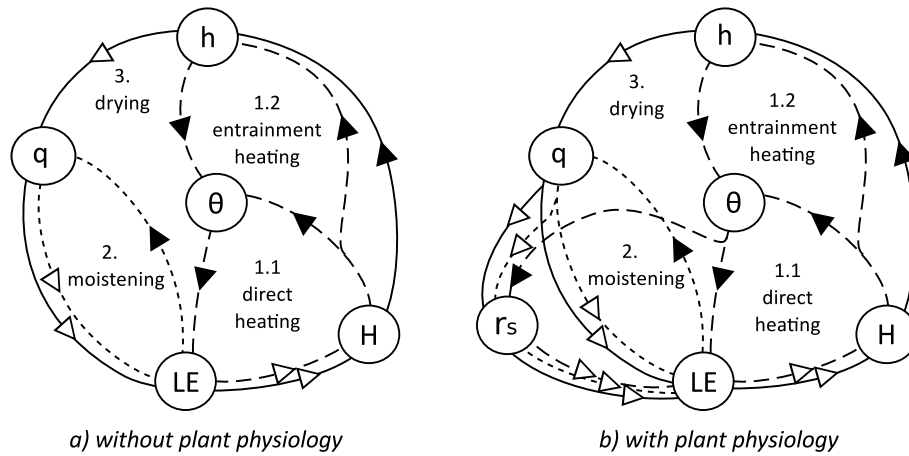


Fig. 2. Overview of the most relevant feedback loops between the land surface and the atmospheric boundary layer for forest and grassland without and with the active role of the plant physiology (left figure comes from van Heerwaarden et al. (2009)). Closed triangles show positive correlations, open triangles negative ones. Each line style describes a distinct feedback loop. LE is the evapotranspiration, H is the sensible heat flux, θ and q are the potential temperature and the specific humidity of the convective boundary layer, h is the height of that layer and r_s is the stomatal resistance.

140 **2 Land-atmosphere coupling over grassland and forest**

The atmospheric control on evapotranspiration works on short time scales, due to the turbulent nature of the trans-175
 port and mixing in the atmospheric boundary layer. Therefore, during daytime heat and moisture are efficiently trans-175
 145 ported away from the surface and mixed throughout this layer on time scales on the order of tens of minutes. Over well-
 watered grasslands, with little dynamics in the stomatal resistance, this leads to a system with three dominant negative feedback loops that are shortly summarized here (see Figure 2). We refer for a complete description to van Heerwaarden
 150 et al. (2009).

First, there is the heating feedback, where heating of the atmosphere, either direct or indirect through entrainment by boundary layer growth, increases the capacity for water and therefore the potential evaporation. Second, there is the drying feedback. Throughout the day the turbulent atmospheric boundary layer grows, and therefore brings in dry air from the free atmosphere above the atmospheric boundary layer. The drying of the air reduces the degree to which the atmospheric capacity for water has been met and therefore also enhances the potential evaporation. Third, the moistening feedback takes into account that the evapotranspiration reduces when the atmosphere moistens due to evapotranspiration. These three feedback loops direct the system towards a state defined as equilibrium evaporation (Raupach, 2000, 2001; van Heerwaarden et al., 2009). In this representation of the system, we conclude that on short time scales, changes
 165 in the actual evapotranspiration rate are driven by changes in the temperature and humidity in the atmospheric boundary layer and therefore in the potential evaporation rate.
 170

Thus far, the feedback loops in the system did not take into account the response of the vegetation to the atmospheric flow and therefore implicitly assumed that the stomatal resistance is constant in time, such that the atmosphere is the only control on evapotranspiration. This, however, is a simplification that only applies to well-watered grassland. For most natural vegetation the feedback loops are more complex and an additional connection is added: the response of the stomatal resistance to the atmospheric temperature and humidity. Leaf stomata are known to react strongly to increasing dryness of the air by letting the trees close their stomata. The stomatal resistance, to which the evapotranspiration rate is inversely proportional, increases thus under a larger vapor pressure deficit (VPD) (Oren et al., 1999). Furthermore, there are indications that vegetation has an optimum temperature beyond which the stomatal resistance decreases (Noilhan and Mahfouf, 1996). The plant physiology has a dramatic effect on the behavior of the system; in the simplified system warming and drying lead to an increase in evapotranspiration, whereas in a coupled system where the stomatal resistance response to the atmosphere, there is a competition between the enhancement of the potential evaporation and the increase in the stomatal resistance. As soon as the latter effect becomes stronger all feedback loops change from negative to positive: more heating and drying lead to a higher stomatal resistance and less evapotranspiration, which in turn leads to more heating and drying. We show in Section 4.2 that the shift of the system from one that evolves towards equilibrium evaporation to one that evolves towards very low evapotranspiration rates leaves a distinct signal in the results.

3 Methods

3.1 Coupled land-atmosphere model

This study uses a simple, but accurate model of the coupled land-atmosphere system that has been explained in detail in van Heerwaarden et al. (2010a). The atmospheric part of the model is a bulk model for the convective boundary layer (Tennekes, 1973). Furthermore, it has a simplified radiation parametrization that provides the incoming short and long wave radiation to the system. The surface energy balance at the land surface is solved using the Penman-Monteith equation (Monteith, 1965) and the heat and moisture transport in the soil is described using a force-restore model (Noilhan and Mahfouf, 1996).

Since this study is about the differences between grassland and forest, we focus here only on the properties that control these differences and how these are implemented in the model. The albedo α is used in the calculation of the net short wave radiation S_{net} following:

$$S_{net} = (1 - cc)(1 - \alpha)S_{in}, \quad (1)$$

where S_{in} is the incoming shortwave radiation and cc is the cloud cover. The albedo influences therefore the amount of net radiation available for the sensible, latent and soil heat flux. Note that we only take the shortwave effect of clouds into account.

The roughness lengths z_{0m} and z_{0h} enter in the calculation of the drag coefficient (Paulson, 1970), to which the aerodynamic resistance r_a , is inversely proportional. The aerodynamic resistance is included in the evapotranspiration calculation:

$$LE \propto \frac{1}{r_a + r_s}, \quad (2)$$

where LE is the latent heat flux or evapotranspiration and r_s the stomatal resistance.

Two main properties determine the calculation of the stomatal resistance r_s : the ratio of the minimal stomatal resistance to the leaf-area index, and the response of the stomata to environmental conditions. The former because it determines to which extent potential evaporation (at $r_s = 0 \text{ s m}^{-1}$) can be met under unstressed conditions (see Eq. 2) and the latter as it takes into account (amongst other things) the previously discussed strong response of tree leaf stomata to vapor pressure deficit. The r_s is calculated following Jarvis (1976):

$$r_s = \frac{r_{s,min}}{LAI} f_1(S_{in}) f_2(w) f_3(VPD) f_4(T) \quad (3)$$

where f_n are correction functions for a certain variable, w is the soil moisture and T is the atmospheric temperature at the vegetation level. The response function f_3 to vapor pressure deficit VPD can be described by:

$$f_3 = e^{g_D VPD} \quad (4)$$

where g_D an empirical constant that describes the strength of the response of the vegetation to the vapor pressure deficit.

The response function f_4 to atmospheric temperature (Noilhan and Mahfouf, 1996) is:

$$f_4 = 1 - 0.0016(298 - T_a)^2 \quad (5)$$

The other correction functions are discussed in van Heerwaarden et al. (2010a).

In the Jarvis model, the correction functions are assumed to be independent of each other. In reality, however, there is a strong correlation between the atmospheric temperature and the vapor pressure deficit, since temperature is the main driver of the VPD under high temperature conditions (van Heerwaarden et al., 2010a). As the correction functions of the Jarvis model and the associated parameters are purely empirical and there exists a correlation between temperature and VPD, tuning of the model does not necessarily gives a unique set of correction functions. This explains the difference between the set of functions among different models that all have shown good performance (Noilhan and Mahfouf, 1996; Ek et al., 2003).

In our set of functions the stomatal resistance of grassland does not respond directly to VPD, but instead it is the temperature correction function f_4 that increases the resistance. Although this may be mechanically inaccurate, since there is evidence that at least some species do appear to be sensitive to VPD (van de Boer et al., 2014), this approach has been shown to work well in atmospheric model studies that consider both grassland and forest (Stap et al., 2014).

3.2 Modeling experiment

In our modeling experiment, we focus on the daytime conditions and the response of vegetation to heat waves on the time scales of turbulence (seconds to minutes). This means that we constrain our model simulations to a single day, as this is long enough to draw conclusions on the response of fast processes. The atmospheric temperature, humidity and wind profiles that we provide to the model are representative for western European summer conditions. An overview of the specific parameters for grassland and forest is shown in Table 1 and a detailed list of all parameters is given in Table A1 in the appendix. A similar approach has been followed in van Heerwaarden et al. (2010b), but then for the Great Plains in the USA.

We tune the cloud cover and the soil moisture of the model such that it produces values of the incoming radiation and partitioning between sensible and latent heat fluxes that are consistent with observations in T10. We stress here that our aim is not to exactly reproduce the data, but rather to demonstrate the behavior of the system and to make an assessment of the most important links in the coupled system. In Figure 4 and onward, we look at the sensitivity of the system to any change in initial temperature and incoming radiation.

Table 1. Model parameters specific for forest and grassland. Values taken from the ECMWF IFS documentation (Cy36r1, Table 8.1) using the mixed crops as the value for grassland and the broadleaf deciduous forest for forest.

variable	description and units	grassland	forest
α	surface albedo [-]	0.21	0.13
Z_{0m}	roughness length for momentum [m]	0.15	2.
Z_{0h}	roughness length for heat and moisture [m]	0.015	2.
$r_{s,min}/LAI$	minimum resistance / leaf area index [$s\ m^{-1}$]	180./3.	175./5.
g_D	exponent for VPD response [-]	0.	0.03

300 After establishing the mean state that is consistent with T10, we continue by performing a sensitivity study on the incoming radiation by varying the cloud cover and the early-morning temperature. In order to maintain realistic atmospheric conditions during the sensitivity experiment, we shift the entire atmospheric potential temperature profile and the near surface soil temperature towards new values, such that the vertical gradients are maintained. Based on this new profile, we perturb the specific humidity, such that we maintain the same initial relative humidity in all our experiments, to allow for a fair comparison. Since the model is fast, we can explore a large number of combinations. Within these simulation results, we locate the heat wave conditions that match the short wave radiation anomaly and temperature anomaly that T10 has reported.

310 Then, in order to understand better the importance of the individual properties that distinguishes forest from grassland in our model (albedo, roughness length, stomatal response to VPD and ratio of the minimal resistance to the leaf area index), we redo our sensitivity study again, but with newly created land use types that resemble grassland with one of the four properties of forest attached to it. With this approach we can estimate the relative importance of each property and the degree to which the different properties weaken or strengthen each other.

325 4 Results

340 4.1 Reproduction of the measurements

The model setup described in Section 3 is able to reproduce the most important characteristics of the measurements. Figure 3 shows the surface energy balance under average forcings and under typical heat wave conditions and can directly be compared Figure 1b and 1d in T10. Since we have chosen those values for incoming short wave radiation and soil moisture contents that reproduce T10's mean state in the best possible way, the match is not surprising. We would like to stress that due to the large variations in soil types and detailed land uses among the different FLUXNET sites, we have chosen a composite value of soil moisture that merely serves to deliver the correct fluxes. Although the role of soil moisture in pro-

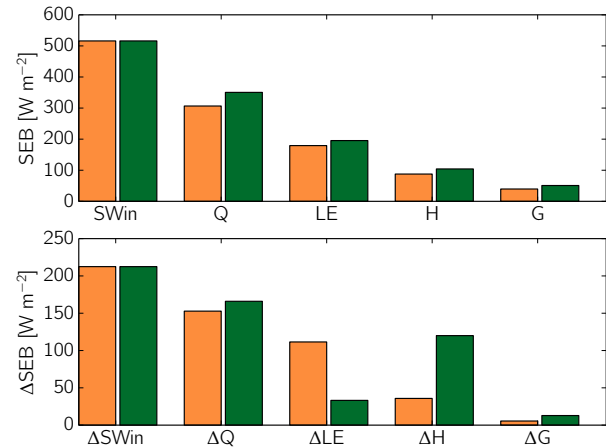


Fig. 3. The surface energy balance (SEB) under standard conditions (top panel) and under heat wave conditions (bottom panel) as computed in the modeling experiment. The values are the 10 h means over the entire duration of the model run. The difference is computed by subtracting the mean state from the heat wave conditions.

longed heat waves is evident, these are outside of the scope of this study and covered in detail elsewhere (T10, Seneviratne et al., 2010; Miralles et al., 2014). The heat wave state, which has been achieved by only perturbing the incoming radiation and the early morning temperature of the mean state, is reproduced well by the model; all modeled anomalies follow the data of T10 and especially the enhanced sensible heat flux over forest of approximately $125\ W\ m^{-2}$ ($121\ W\ m^{-2}$ in T10) is reproduced well. This finding implies that the model, and therefore parametrizations in existing numerical weather prediction and climate models, are able to reproduce the response of forests to perturbations in the incoming radiation and temperature, even without accounting for possible soil moisture differences between reference and heatwave conditions

4.2 The sensitivity of grassland and forest to incoming short wave radiation and temperature

Figures 4 and 5 show the results of the entire sensitivity study of which the day that is contained in Figure 3a has been perturbed. Figure 4 illustrates the sensitivity of the net radiation, the evapotranspiration and the sensible heat flux to the incoming radiation and the early morning temperature for both forest and grassland.

The surface energy balance and the atmospheric properties of grassland change monotonically under changes in the radiation and the early-morning temperature, whereas those of forest displays more complex behavior. As we already have hypothesized in Section 2, grassland mostly responds to the changes in the potential evaporation, an increase in temperature or radiation automatically results in an increase in evapotranspiration, with a uniform sensitivity over the majority of the parameter range. The net radiation is logically mostly sensitive to changes in the incoming short wave radiation. Nonetheless, a slight reduction in net radiation is observed with increasing temperature (5 W m^{-2} over the entire temperature range), which is related to the increase in surface temperature and the consequent increase in the outgoing long wave radiation.

Forest has a maximum in evapotranspiration and a minimum in the sensible heat flux for given high values of incoming radiation (located at an early morning temperature of 297 K for an incoming radiation of 500 W m^{-2} , until a temperature of 291 K for 750 W m^{-2}). At low early-morning temperatures, the increase in potential evaporation related to the higher temperatures is the dominant effect. However, the decrease in actual evapotranspiration due to the higher stomatal resistance is the strongest effect at higher temperatures, resulting in a reduction of evapotranspiration with an increase in early morning temperature, similar as shown in the observations in Figure 1b. Over forest, the change in sensible heat flux with early morning temperature is non-monotonic as well.

In order to explain the observations shown in Figure 1, we have marked (black dotted lines, indicating the 93 to 105 W m^{-2} interval) the combinations of incoming short wave radiation and initial temperature that give a constant sensible heat flux over grassland in the same range as that in Figure 1. Within this range, the sensible heat flux of forest increases in the direction of heatwave conditions (high temperature and incoming radiation) from approximately 115 W m^{-2} to values more than 200 W m^{-2} while moving to higher values for incoming radiation and initial temperature. This behavior matches very well with what is found in Figure 1 and reconfirms the feedback mechanisms discussed in Section 2.

The differences in surface energy balance between grassland and forest are reflected in the atmospheric boundary layer characteristics (Figure 5). The shaded region shows the maximum two-meter temperature that is achieved dur-

ing the day. Under conditions of low early-morning temperatures and a small amount of incoming radiation, which are found in the bottom left of the plots, the maximum two-meter temperature is comparable for grassland and forest ($\sim 293 \text{ K}$ for an early morning temperature of 283 K and an incoming shortwave radiation of 500 W m^{-2}). While we move towards the top right in the plots, thus to higher early-morning temperatures and more incoming shortwave radiation, the maximum temperature over forest increases considerably faster over forest (313 K) than over grassland (308 K). In Figure 4, we have seen that this is due to an increase in the sensible heat fluxes over forest that is not found over grassland.

The changes in the VPD show the increased drying of the atmosphere over the forest (solid blue lines, Figure 5). While grassland has a range from 12 to 26 hPa over the entire parameter space, the VPD over the forest increases from 13.5 to 38 hPa, which is a much wider range than that over grassland.

The occurrence of a maximum evapotranspiration rate with increasing temperature is reflected in the achieved atmospheric boundary layer heights (dashed red lines, Figure 5). Grassland shows again a monotonic behavior; the boundary layer height increases with increasing incoming short wave radiation due to the extra available energy, whereas the boundary layer height decreases under rising early-morning temperatures, due to the shift of energy from sensible to latent heating.

The achieved boundary layer heights over forest show a curved line that displays a minimum with respect to early-morning temperature close to values of 296 K for high values of incoming shortwave radiation. This minimum is directly related to the maximum evapotranspiration that was found in Figure 4 and the result of the vegetation enforced feedback mechanism that is also responsible for the minimum in sensible heat flux found over forest.

4.3 Unraveling the feedback mechanisms

In the previous section we have shown that we are able to reproduce the measurements of T10 with our model. The aim of the current section is to find the relative importance of each of the differences in properties between grassland and forest in creating the big difference between the two land use types that was found in the measurements of T10. With our model we compare the response of the coupled system to perturbations in incoming radiation and temperature for a set of land use types. This set contains grassland and forest itself, but also the newly created virtual land use types that have the properties of grassland, but with one of the properties replaced by that of forest, such that we can assess the influence of each forest property separately.

Figure 6 shows the difference between grassland and forest, the influence of the four properties separately and the importance of the interaction between the feedbacks. Figure 6a shows the difference in evapotranspiration, maximum tem-

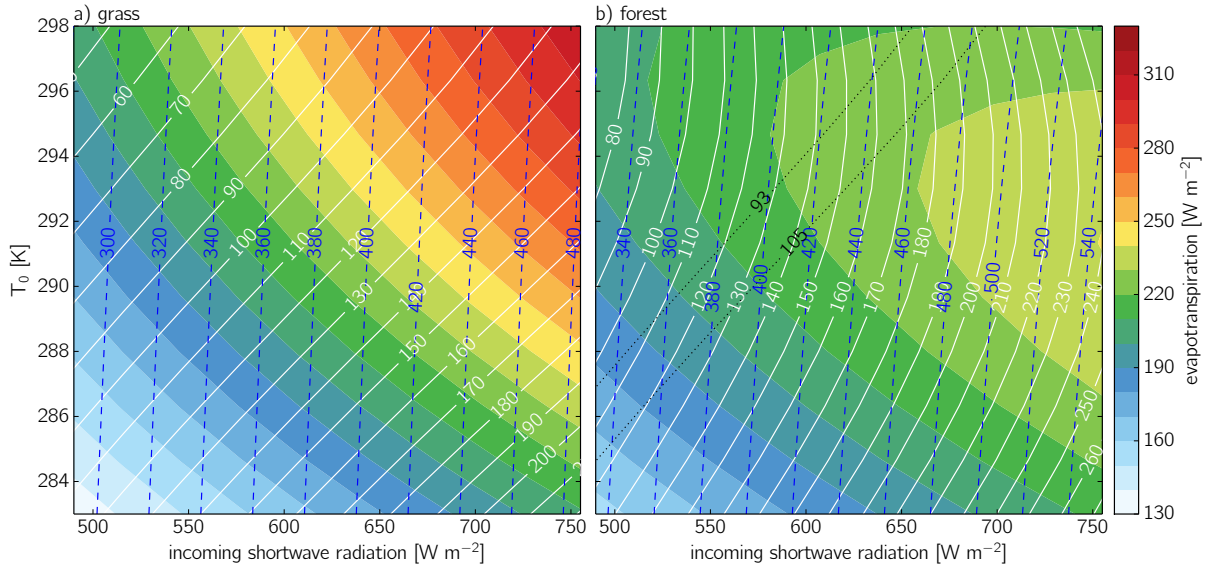


Fig. 4. Evapotranspiration or latent heat flux (shades), sensible heat flux (white solid lines) and net radiation (blue dashed lines). The values are the 10 h means over the entire duration of the model run. The black dotted lines correspond to the range in which grassland gives a constant sensible heat flux with similar magnitudes as those in the observations in Figure 1.

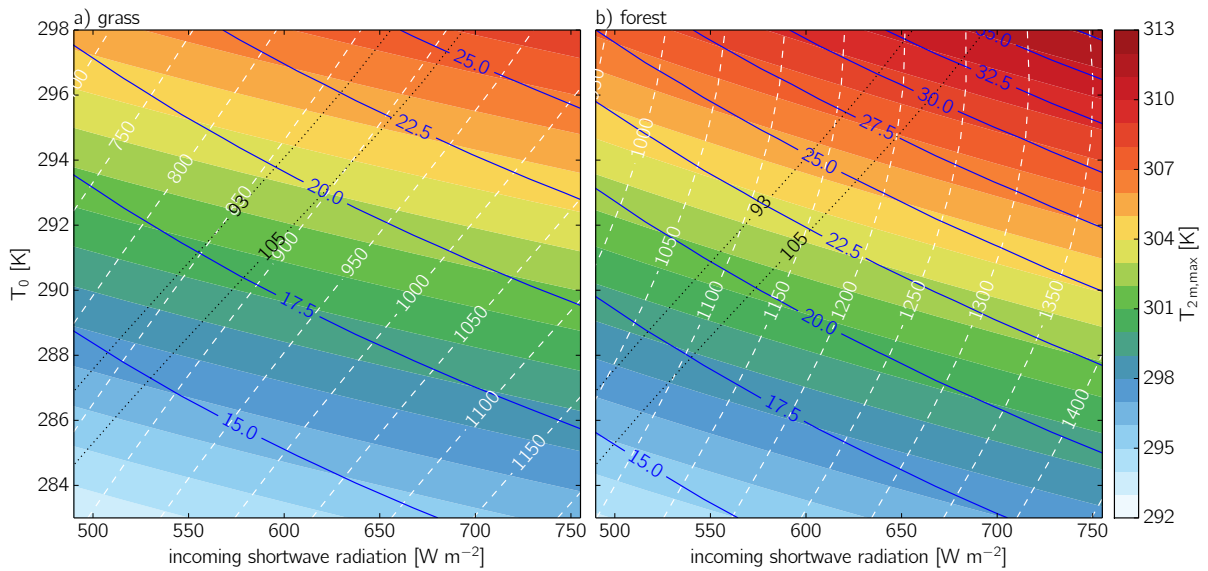


Fig. 5. Maximum temperatures (shades), vapor pressure deficit (blue solid lines) and boundary layer height (white dashed lines). The values for the VPD (hPa) and the boundary layer height (m) are the 10 h means over the entire duration of the model run, the maximum 2 m temperature is the maximum over the duration. The black dotted lines correspond to the range in which grassland gives a constant sensible heat flux with similar magnitudes as those in the observations in Figure 1.

perature and net radiation that is the result of subtracting the values of grassland from those of forest, which are shown in Figures 4 and 5.

The first property that we take into consideration is the albedo (Figure 6b). The most importance change to the system if the albedo of forest is attributed to the grassland is

the increase in net radiation for forest, because it has a lower albedo than grassland. The difference increases from 36 to 56 $W m^{-2}$ over the range of shortwave radiation on the horizontal axis, where forest, with its lower albedo, converts more of the extra incoming short wave radiation to net radiation. The evapotranspiration ($\sim 25 W m^{-2}$) and the maxi-

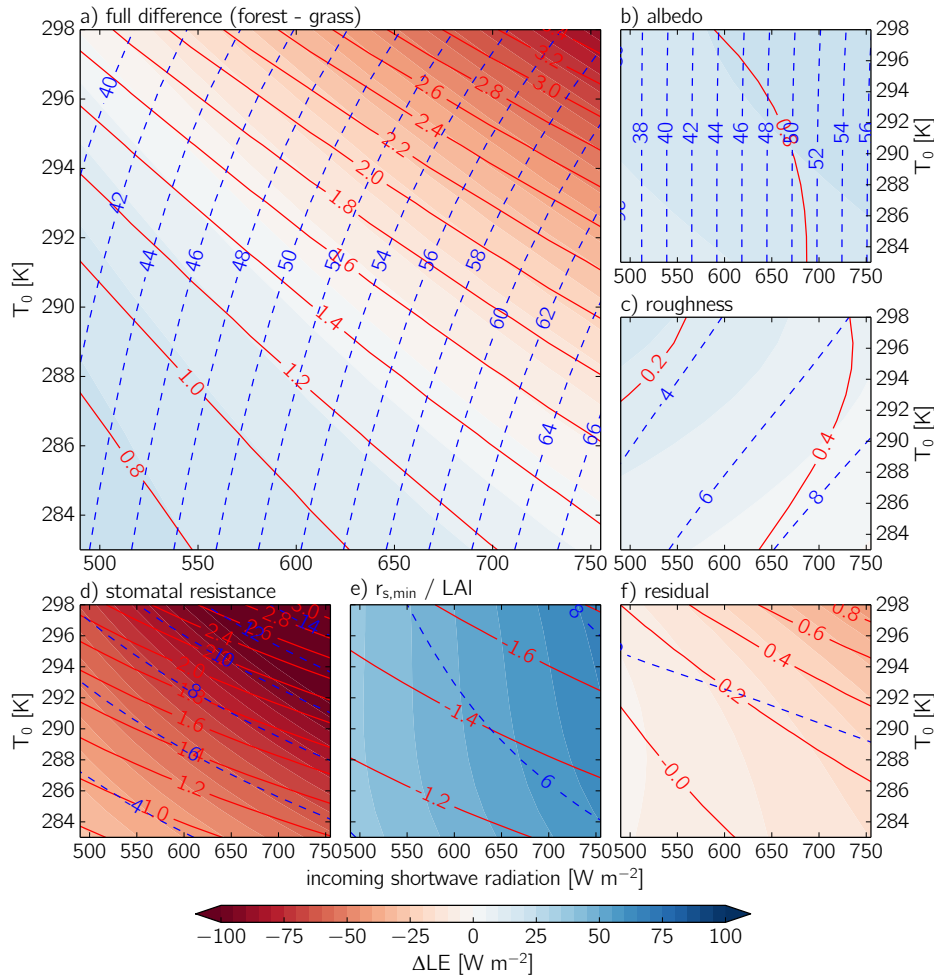


Fig. 6. Difference in evapotranspiration (shades), maximum temperature (red solid line) and net radiation (blue dashed line) between forest and grassland as a function of initial temperature and incoming shortwave radiation. Small panels indicate the contribution of individual processes/parameters, such that the values in the small panels sum up to the value in the large panel. The values for evapotranspiration and net radiation are the 10 h means over the entire duration of the model run, the maximum 2 m temperature is the maximum over the entire duration.

475 mum temperature (~ 0.8 K) show an increase over the entire parameter range, but have a low sensitivity to changes in the radiation or early-morning temperature.

480 The second property is roughness (Figure 6c). If we increase the roughness of the grassland to that of forest, then the evapotranspiration, maximum temperature and net radiation are affected. In all three variables, the strongest changes 495 occur under a low early morning temperature and a high incoming shortwave radiation, because here the sensible heat flux is the highest. We suggest that the changes are the effect of a sequence of events that starts with an increased mixing near the surface, due to the higher roughness. Subsequently, 500 the near-surface temperature resembles more that of its overlying atmosphere and drops. Then, the outgoing long wave radiation decreases, resulting in an increase of the available energy for the sensible and latent heat flux. This results in a

slightly increased evapotranspiration and sensible heat flux, with an eventual rise in maximum temperature despite the stronger mixing. This interpretation is applicable to the entire range of incoming radiation and early-morning temperatures. All in all, the sensitivity of the system to roughness is relatively low compared to the other properties, which is in line with the previous findings of Hill et al. (2008).

The third property that we study is the response of the stomatal resistance to atmospheric temperature and humidity, thus the fast physiological processes in the vegetation (Figure 6d). We already identified the closure of stomata as a potential mechanism to strongly reduce the evapotranspiration (Section 2) and Figure 6 delivers a quantitative confirmation of this hypothesis. Without major modifications to the net radiation, the replacement of the correction functions of grassland by those of forest results in a large drop in evap-

505 otranspiration (up to 100 W m^{-2}) and a consequent increase
in the maximum temperature (more than 2.6 K) through an
enhanced sensible heat flux over the entire parameter space.
The strength of the drying of the atmosphere is reflected in 560
the larger VPD over forest than grassland (more than 15 hPa).

510 The fourth and last property included in the study is the
ratio of minimum stomatal resistance to the leaf-area index
(see Equation 3), which is a measure of the maximal poten-
tial of the plants to transpire under unstressed soil moisture 565
conditions (Figure 6e). Since forest has a lower value, it has
515 a lower stomatal resistance under unstressed conditions and
therefore higher evapotranspiration rates (30 to 50 W m^{-2}
more than grassland). Hill et al. (2008) already pointed out
the importance of the leaf area index. The higher evapotran- 570
spiration rate results in significantly lower maximum temper-
520 atures over forest (more than 1.2 K less than grassland). The
net radiation is fairly insensitive to this parameter.

In order to estimate to which extent the properties counter-
act or strengthen the effect of the other properties, we have 575
subtracted the four individual effects from the total differ-
525 ence, so that a residual is acquired (Figure 6f). We find that
the reduction of evapotranspiration under increasing temper-
ature and radiation can be more than 50 W m^{-2} larger than
the sum of the four individual components. We hypothesize 580
that the increased reduction is related to strong interactions
530 between the effects of albedo and that of the physiological
processes. Whereas the extra energy provided by the lower
albedo is added to the evapotranspiration in Figure 6b, this
extra energy ends up in the heating in the residual (Figure 6f). 585
Here, the system has entered the positive feedback loop (Fig-
535 ure 2), where additional energy leads to an enhanced drying
and heating. The additional net radiation of approximately
 50 W m^{-2} , results in an enhanced reduction in evapotran-
590 spiration of the same amount of energy and an additional
540 increase in the maximum temperature of 1 K, almost 25 %
of the total difference. The slight increase in net radiation,
is most likely related to the interplay between the proper-
ties related to the vegetation response and the roughness. In
this case, the increase in roughness counteracts the highly 595
enhanced surface temperature that is the effect of the phys-
545 iological processes. Therefore, there is a slight reduction
in the outgoing long wave radiation and a corresponding small
increase in the net radiation.

5 Conclusions

We have studied the differences in land-atmosphere coupling
550 between grassland and forest during the onset of heat waves 605
by means of a modeling experiment in which a typical sum-
mer day for Western European conditions has been analyzed
under normal and under heat wave conditions. With a sim-
ple, but accurate conceptual model that contains the essen-
555 tial processes in the coupled land-atmosphere system (van 610
Heerwaarden et al., 2010a), we are able to reproduce the ob-

servations of Teuling et al. (2010) (T10) who showed higher
temperatures over forest than over grassland during the early
stages of heat waves.

In addition to reproducing the data of T10, we have per-
formed a sensitivity study on the response of forest and
grassland to perturbations of the early-morning tempera-
ture and radiation in order to mimic the forcings that cor-
respond to heat waves. From this analysis we have learned
that both grassland and forest display a monotonically in-
creasing evapotranspiration and sensible heat flux under in-
creasing incoming shortwave radiation, forced by an increase
in potential evaporation. The reaction to a rise in early-
morning temperature is more complex. Although grassland
shows monotonic increases in evapotranspiration and mono-
tonic decreases in sensible heat flux and atmospheric bound-
ary layer height under increasing early-morning tempera-
tures, forest displays more complex behavior; beyond a criti-
cal threshold, the effects of the atmospheric temperature and
humidity on stomatal closure are stronger than the effects on
the potential evaporation. Therefore, the evapotranspiration
no longer increases but decreases with increasing tempera-
ture, resulting in an increasing sensible heat flux, maximum
temperature and atmospheric boundary layer height.

Furthermore, we have repeated the sensitivity study not
only for forest and grass, but also for a series of virtual land
use types that resemble grassland with one of its properties
replaced by the corresponding property of forest. Here, it
was found that strong temperature increase over forest is pri-
marily driven by the feedback mechanism that leads to an
increasingly fast shutdown of evapotranspiration (Figure 2),
related to the stomatal closure of the leaves of trees under heat
wave conditions. While this finding is not a surprise on itself,
our results show that all properties are essential in explaining
the results of T10. Mostly the lower albedo of forest plays
a crucial role; Without the fast physiological processes of
the vegetation, the lower albedo mostly enhances the evap-
otranspiration by providing more energy, whereas all the ex-
tra energy is converted into sensible heat when the stomatal
response to temperature and humidity is present.

Our results are mainly valid for the onset of heat waves
and we expect that as soon as the evapotranspiration fluxes
start depleting the soil moisture reservoirs, the evolution of
the soil moisture takes over as the most crucial aspect of the
system. It is interesting, however, that soil moisture differ-
ences are not a prerequisite for the reproduction of the results
in T10), indicating that short-term land-atmosphere interac-
tion rather than soil moisture can explain the observed flux
differences.

A logical extension of this study of idealized land-atmos-
phere coupling is an investigation of the exact role of land-
surface heterogeneity. In our study, we have assumed that
the surface and the atmosphere are in equilibrium with each
other, which requires areas of uniform land use with a ra-
dius of at least tens of kilometers (Mahrt, 2000). Many of the
Western-European forests are smaller than this, and there-

fore, the air over forests partly resembles that of grasslands. The relatively moist air coming from the strongly evaporating grassland could largely suppress the effects of the VPD-related feedback (Figure 2), making the high roughness of forest relatively more important. This could explain why several studies have reported lower surface temperatures in forests under heat wave conditions.

To conclude, our results suggest that the high temperatures over forest compared to grassland that T10 found are mainly driven by the fast response of the vegetation to the temperature and humidity of the atmosphere. The good news is that the simple parametrizations that are used in our model and in many of the numerical weather prediction models are able to reproduce the heat wave response. Nonetheless, the large magnitude of the temperature rise over forest is the result of a complex interplay of land-surface and atmospheric boundary layer processes. The downside of the type of model that we used is that its parameterizations of stomatal resistance are empirical, and that a fully mechanistic model for stomatal resistance is lacking. This casts doubt on the validity of such models for studies of future climates, where situations can occur that are outside of the tuning range. Our study therefore stresses the need for mechanistic models of physiological processes in plants and for a close collaboration between the biological and hydro-meteorological sciences.

Acknowledgements. AJT acknowledges financial support from The Netherlands Organization for Scientific Research through Veni grant 016.111.002. The authors acknowledge the constructive comments of Linda Schlemmer on this manuscript.

Appendix A

Model parameters

Table A1 contains an overview of all chosen parameters for our model setup. We have chosen 50°N as the representative latitude for central Western Europe, the region that T10 studies. Our simulations make use of idealized atmospheric profiles that match the climatology. We maintain the early morning relative humidity of our simulations, such that the specific humidity profile changes with the temperature. Our soil parameters describe a standard loamy soil.

References

Anderson, R. G., Canadell, J. G., Randerson, J. T., Jackson, R. B., Hungate, B. A., Baldocchi, D. D., Ban-Weiss, G. A., Bonan, G. B., Caldeira, K., Cao, L., Diffenbaugh, N. S., Gurney, K. R., Kueppers, L. M., Law, B. E., Luyssaert, S., and O'Halloran, T. L.: Biophysical considerations in forestry for climate protection, *Frontiers in Ecology and the environment*, 9, 174–182, doi:10.1890/090179, 2010.

Bonan, G. B.: Forests and climate change: forcings, feedbacks, and the climate benefits of forest, *Science*, 320, 1444–1449, doi:10.1126/science.1155121, 2008.

Brilli, F., Hoernagl, L., Hammerle, A., Haslwanter, A., Hansel, A., Oreo, F., and Wohlfahrt, G.: Leaf and ecosystem response to soil water availability in mountain grasslands, *Agric. For. Meteorol.*, 151, 1731–1740, 2011.

Christidis, N., Stott, P. A., Hegerl, G. C., and Betts, R. A.: The role of land use change in the recent warming of daily extreme temperatures, *Geophys. Res. Lett.*, 40, 589–594, doi:10.1002/grl.50159, 2013.

Davin, E. L. and de Noblet-Ducoudré: Climatic impact of global-scale deforestation: radiative versus nonradiative processes, *J. Climate*, 23, 97–112, doi:10.1175/2009JCLI3102.1, 2010.

Ek, M. B., Mitchell, K. E., Lin, Y., Rogers, E., Grunmann, P., Koren, V., Gayno, G., and Tarpley, J. D.: Implementation of NOAA land surface model advances in the National Centers for Environmental Prediction operational mesoscale Eta model, *J. Geophys. Res.*, 108, D22, 8851, doi:10.1029/2002JD003296, 2003.

Fischer, E. M., Seneviratne, S. I., Lüthi, D., and Schär: Contribution of land-atmosphere coupling to recent European summer heat waves, *Geophys. Res. Lett.*, 34, L06707, doi:10.1029/2006GL029068, 2007.

Hill, T. C., Williams, M., and Moncrieff, J. B.: Modeling feedbacks between a boreal forest and the planetary boundary layer, *J. Geophys. Res.*, 113, D15122, doi:10.1029/2007JD009412, 2008.

IPCC: Climate Change 2013: The Physical Science Basis. Contribution of Working Group I to the Fifth Assessment Report of the Intergovernmental Panel on Climate Change, Cambridge University Press, Cambridge, United Kingdom and New York, NY, USA, 2013.

Jarvis, P. G.: The interpretation of the variations in leaf water potential and stomatal conductance found in canopies in the field, *Philos. Trans. Roy. Soc. London*, 273B, 593–610, 1976.

Mahrt, L.: Surface heterogeneity and vertical structure of the boundary layer, *Bound.-Layer Meteorol.*, 96, 33–62, 2000.

Miralles, D. G., van den Berg, M. J., Teuling, A. J., and de Jeu, R. A. M.: Soil moisture-temperature coupling: a multi-scale observational analysis, *Geophys. Res. Lett.*, 39, L21707, doi:10.1029/2012GL053703, 2012.

Miralles, D. G., Teuling, A. J., van Heerwaarden, C. C., and de Arelano, V.-G.: Mega-heatwave temperatures due to combined soil desiccation and atmospheric heat accumulation, *Nature Geoscience*, 7, 345–349, doi:10.1038/ngeo2141, 2014.

Monteith, J. L.: Evaporation and environment, *Symp. Soc. Exp. Biol.*, XIX, 1965.

Monteith, J. L.: A reinterpretation of stomatal response to humidity, *Plant, Cell and Environment*, 18, 357–364, 1995.

Noilhan, J. and Mahfouf, J.-F.: The ISBA land surface parameterization scheme, *Glob. Plan. Change*, 13, 145–159, 1996.

Oren, R., Sperry, J. S., Katul, G. G., Pataki, D. E., Ewers, B. E., Phillips, N., and Schäfer, K. V. R.: Survey and synthesis of intra- and interspecific variation in stomatal sensitivity to vapour pressure deficit, *Plant, Cell and Environment*, 22, 1515–1526, 1999.

Paulson, C. A.: The mathematical representation of wind speed and temperature profiles in the unstable atmospheric surface layer, *J. Applied Met.*, 9, 857–861, 1970.

Raupach, M. R.: Equilibrium evaporation and the convective boundary layer, *Bound.-Layer Meteorol.*, 96, 107–141, 2000.

Table A1. Initial and boundary conditions for all model runs.

variable	description and unit	values
P_0	surface pressure [Pa]	101300.
lat	latitude [deg]	50 N
lon	longitude [deg]	0 E
doy	day of the year [-]	182.
t_{start}	start time of simulation in local time [h]	7
t_{end}	end time of simulation in local time [h]	17
cc	cloud cover [-]	cc_{input}
w_g	volumetric water content top soil layer [$m^3 m^{-3}$]	0.235
w_2	volumetric water content deeper soil layer [$m^3 m^{-3}$]	0.235
c_{veg}	vegetation fraction [-]	0.9
T_{soil}	temperature top soil layer [K]	$T_{input} - 3$
T_2	temperature deeper soil layer [K]	$T_{input} - 2$
a	Clapp and Hornberger retention curve parameter [-]	0.219
b	Clapp and Hornberger retention curve parameter [-]	4.90
p	Clapp and Hornberger retention curve parameter [-]	4.
CG_{sat}	saturated soil conductivity for heat [$K m^{-2} J^{-1}$]	$3.56e-6$
w_{sat}	saturated volumetric water content [$m^3 m^{-3}$]	0.472
w_{fc}	volumetric water content field capacity [$m^3 m^{-3}$]	0.323
w_{wilt}	volumetric water content wilting point [$m^3 m^{-3}$]	0.171
$C1_{sat}$	Coefficient force term moisture [-]	0.132
$C2_{ref}$	Coefficient restore term moisture [-]	1.8
LAI	leaf area index [-]	see Table 1
$r_{s,min}$	minimum resistance transpiration [$s m^{-1}$]	
z_{0m}	roughness length for momentum [m]	
z_{0h}	roughness length for heat and moisture [m]	
α	surface albedo [-]	
g_D	exponent for VPD response	
h	initial ABL height [m]	200.
θ	initial mixed layer potential temperature [K]	T_{input}
$\Delta\theta$	initial temperature jump at h [K]	$T_{input}+5$
γ_θ	free atmosphere potential temperature lapse rate [$K m^{-1}$]	0.006
A_{θ_v}	entrainment ratio for virtual potential temperature[-]	0.2
q	initial mixed layer specific humidity [$kg kg^{-1}$]	RH = 0.7
Δq	initial specific humidity jump at h [$kg kg^{-1}$]	-0.002
u	initial mixed layer wind speed [$m s^{-1}$]	7.
ug	geostrophic wind speed [$m s^{-1}$]	10.

- Raupach, M. R.: Combination theory and equilibrium evaporation, *Quart. J. Roy. Meteor. Soc.*, 127, 1149–1181, 2001. 735
- 720 Seneviratne, S. I., Corti, T., Davin, E., Hirschi, M., Jaeger, E. B., Lehner, I., Orlowsky, B., and Teuling, A.: Investigating soil moisture-climate interactions in a changing climate: A review, *Earth-Sci. Rev.*, 99, 125–161, doi:10.1016/j.earscirev.2010.02.004, 2010. 740
- 725 Stap, L. B., van den Hurk, B. J. J. M., van Heerwaarden, C. C., and Neggers, R. A. J.: Modelled contrast in the response of the surface energy balance to heatwaves for forest and grassland, *J. Hydrometeorol.*, doi:10.1175/JHM-D-13-029.1, 2014.
- Streck, N. A.: Stomatal response to water vapor pressure deficit: 745 an unsolved issue, *Current Agricultural Science and Technology*, 2012.
- Tennekes, H.: A model for the dynamics of the inversion above a convective boundary layer, *J. Atmos. Sci.*, 30, 558–567, 1973.
- Teuling, A. J., Seneviratne, S. I., Stöckli, R., Reichstein, M., Moors, E., Ciaia, P., Luyssaert, S., van den Hurk, B., Ammann, C., Bernhofer, C., Dellwik, E., Gianelle11, D., Gielen, B., Grünwald, T., Klumpp, K., Montagnani, L., Moureaux, C., Sottocornola, M., and Wohlfahrt, G.: Contrasting response of European forest and grassland energy exchange to heatwaves, *Nature Geoscience*, doi:10.1038/NGEO950, 2010.
- van de Boer, A., Moene, A. F., Graf, A., Simmer, C., and Holtslag, A. A. M.: Estimation of the refractive index structure parameter from single-level daytime routine weather data, *Applied Optics*, 2014.
- van Heerwaarden, C. C., Vilà-Guerau de Arellano, J., Moene, A. F., and Holtslag, A. A. M.: Interactions between dry-air entrainment, surface evaporation and convective boundary layer development, *Quart. J. Roy. Meteor. Soc.*, 135, 1277–1291, doi:10.1002/qj.431, 2009.

- 750 van Heerwaarden, C. C., Vilà-Guerau de Arellano, J., Gounou, A.,
Guichard, F., and Couvreur, F.: Understanding the daily cycle of evapotranspiration: a method to quantify the influence of forcings and feedbacks, *J. Hydrometeor.*, 11, 1405–1422, doi:10.1175/2010JHM1272.1, 2010a.
- 755 van Heerwaarden, C. C., Vilà-Guerau de Arellano, J., and Teuling, A. J.: Land-atmosphere coupling explains the link between pan evaporation and actual evapotranspiration trends in a changing climate, *Geophys. Res. Lett.*, 37, L21 401, doi:10.1029/2010GL045374, 2010b.
- 760 Vilà-Guerau de Arellano, J., van Heerwaarden, C. C., and Lelieveld, J.: Modelled suppression of boundary-layer clouds by plants in a CO₂-rich atmosphere, *Nature Geoscience*, 5, 701–704, doi:10.1038/NGEO1554, 2012.
- 765 Zaitchik, B. F., Macalady, A. K., Bonneau, L. R., and Smith, R. B.: Europe's 2003 heat wave: A satellite view of impacts and land-atmosphere feedbacks., *Int. J. Climatol.*, 26, 743–769, 2006.